MEMS-based Coulter counter for cell counting and sizing using multiple electrodes

2010 J. Micromech. Microeng. 20 085035

(http://iopscience.iop.org/0960-1317/20/8/085035)

IOP PUBLISHING JOURNAL OF MICROMECHANICS AND MICROENGINEERING

J. Micromech. Microeng. **20** (2010) 085035 (8pp) doi:10.1088/0960-1317/20/8/085035

MEMS-based Coulter counter for cell counting and sizing using multiple electrodes

Y Wu[1], J D Benson[2], J K Critser[3] and M Almasri[1]

[1] Department of Electrical and Computer Engineering, College of Engineering, University of Missouri, Columbia, MO 65211, USA
[2] Department of Mathematics, College of Arts and Science, University of Missouri, Columbia, MO 65211, USA
[3] Comparative Medicine Center, College of Veterinary Medicine, University of Missouri, Columbia, MO 65211, USA

E-mail: almasrim@missouri.edu

Received 7 May 2010, in final form 18 June 2010
Published 21 July 2010
Online at stacks.iop.org/JMM/20/085035

Abstract

A novel MEMS-based Coulter counter is designed, fabricated and tested in this paper. The Coulter counter is used for detection and monitoring the impedance changes of cells as a function of time after they are mixed with different experimental extracellular environments. The device consists of a multilayer of the SU-8 microchannel which is divided into a passive mixing region, a focusing region using negative dielectrophoretic forces and a measuring region by multiple electroplated vertical electrode pairs. The devices were tested with both fluidic and electrical functionality using dyed fluids, microbeads with different dimensions suspended in saline water and fibroblast cells in anisosmotic phosphate buffered saline. The results are presented and discussed. The device ultimately aims at testing time-sensitive cell characteristics after exposure to different extracellular media with enhanced sensitivity.

(Some figures in this article are in colour only in the electronic version)

1. Introduction

Detection and classification of cells is an important aspect of medical research in diagnosis and treatment of diseases at the cellular level. One popular method used in cell research is to grow cells on-chip surfaces to characterize them with electrochemical and physical sensors [1]. Another method is to suspend cells and flow them with media through a micro-fluidic channel. Electronic particle counters (EPCs) such as the Coulter counter are standard diagnostic devices widely used in laboratory medicine and pathology [2]. These devices are used to perform rapid, accurate analysis of blood, and other cells and tissues. An example of these analyses is the complete blood count (CBC) which is used to determine the number or proportion of white and red blood cells in the body. They are also used to characterize cells in terms of their size, and other properties that are important to understand for optimization of methods to store them at low temperatures (cryopreservation) [3]. These methods are essential for transfusion, transplantation and reproductive medicine. Commercially available EPC such as Coulter counters have a number of limitations. First, they are relatively large (about the size of a large desktop printer). Due to their rather large size, they are configured to require relatively large sample volumes. This sample volume requirement limits the ability to process samples more rapidly and severely limits measurement of time-sensitive cell characteristics (e.g. changes in volume in response to changes in solute concentrations). Moreover, this sample size requirement necessitates minimal cell counts on the order of 10^4 to 10^5, an impractical requirement for many cell types and imposes time-to-measurement constraints when measurements are made in non-physiologic media. These sample size and time constraints are detrimental to accurate dynamic volume measurements for some cell types [4, 5]. For example, mouse and rat spermatozoa are available in relatively small numbers and these cells adjust volumetrically very

quickly to anisosmotic environments, equilibrating in less than 10 s in many cases making traditional Coulter counter methods difficult or impossible to implement. While typically being available in large numbers, red blood cells similarly rapidly adjust volumetrically to anisosmotic environments making measurements of water and solute permeability parameters impossible with existing Coulter counter technology.

Several groups have successfully demonstrated miniaturized Coulter counters with various designs using micromachining technology [6–15]. Miniaturized Coulter counters provide many advantages including significantly reduced sample volume, low cost, low power consumption and portability [16]. These micromachined Coulter counters are designed to measure impedance of cells using one or two electrode pairs and thus may only be used for cell counting purposes and static cell sizing. Coulter counters generally employ a focusing mechanism to prevent clogging of the Coulter channel and electrode pair for impedance measurement as a means for cell counting. The cells are focused into a tight stream using hydrodynamic focusing [17–22], dielectrophoresis (DEP) focusing [23, 24] and by means of geometric design [8]. Several particle and cell detection techniques have been used which include optical techniques based on fluorescence detection [24, 25] and electrical techniques including dc impedance sensing which was first invented by Wallace H Coulter [26], ac impedance sensing [27, 28], metal-oxide–semiconductor field-effect transistor (MOSFET) which detects the particles by monitoring the MOSFET drain current modulation [29], radio frequency reflectometer [13] and capacitance measurements [30, 31].

The objective of this paper is to develop a MEMS-based Coulter counter that can ultimately be used to detect and monitor dynamic cell impedance changes as a function of time in response to mixing isolated cell populations with different extracellular media by using a sequence of ten electrode pairs. In this paper, we report the detection of latex microbeads with a diameter of 5 μm, 10 μm and 15 μm, and fibroblast cells with a diameter of 19 μm, using series of vertical electrodes and through impedance measurement. It also reports on cell mixing efficiency using a passive mixer, and focusing of cells using DEP.

2. Theoretical background

The MEMS Coulter counter is based on the use of three phenomena: passive mixing of the extracellular media, negative dielectrophoretic focusing of the cells and electrical impedance-based sensing mechanism. A three-dimensional schematic of the MEMS Coulter counter is shown in figure 1. These phenomena are explained in the following section.

2.1. Passive mixing of the reagents

The MEMS Coulter counter is designed to monitor cellular volumetric change after a change in the composition of the extracellular solution within 0.5 s from the start of mixing and up to 10–15 s. For example, red blood cells adjust volumetrically very quickly to anisosmotic environments. The volumetric changes of cells are due to the net movements of water between the cells and surrounding interstitial fluids, which are determined by the osmolalities of these two compartments [32]. If the osmolality of the interstitial fluid increases, water must leave the cells and hence cell volume decreases. In contrast, fluid must enter the cells and the cell volume increases as osmolality decreases. Therefore, the cells should be mixed very well with specific different extracellular media before their impedance are measured. Thus, the mixing region of the Coulter counter is designed with a passive mixer which allows chaotic mixing of two different extracellular media and cells in a serpentine-shape channel to achieve sufficient fluid mixing efficiency. The two-dimensional serpentine shape mixer is selected because it is relatively easy and simple to implement. The quality of mixing can be evaluated by observing color intensity variation of two dyes with different colors as they flow through the mixer and just before the entrance of the Coulter channel. The mixing efficiency is an important factor that determines the sensitivity of the system and can be determined by analyzing captured images after mixing using image processing.

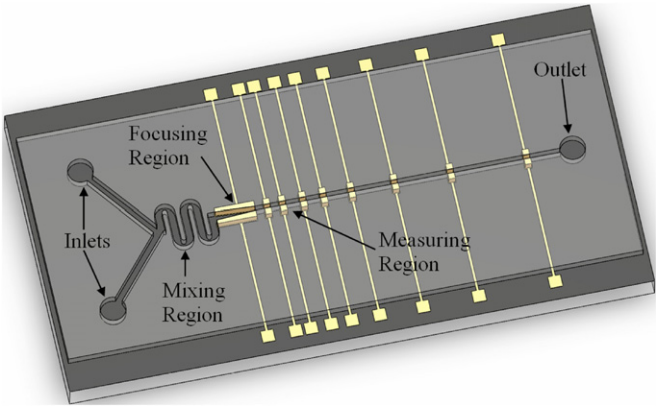

Figure 1. (*a*) Three-dimensional schematic of the MEMS Coulter counter; (*b*) magnified view of the mixing, focusing region and measuring region.

2.2. Dielectrophoretic focusing

DEP is the translational motion of a particle in a suspending medium under the influence of a non-uniform ac electric field [33]. It is used in microfluidic system to enable various manipulations of micro/nano particles and cells such as separation, trapping, assembling and transportation [34, 35]. The phenomenon of negative DEP is employed to focus the cells to the center of the channel as a single line. Thus, cells enter the Coulter channel one by one without clogging it. A non-uniform ac electric field induces a dipole moment in a neutral particle, exerting the force on the particle either to a region of maximum or minimum electric field strength. Two factors determine driving direction: permittivity of the particle compared with that of the medium surrounding the particle and the frequency of the applied electric field. The DEP force (F_{DE}) acting on a spherical particle of radius (r) subjected to non-uniform electric field (E) is given by

$$F_{\mathrm{DE}} = 2\pi r^3 \,\mathrm{Re}[f(\varepsilon_p^*, \varepsilon_m^*)]\nabla|\vec{E}^2| \qquad (1)$$

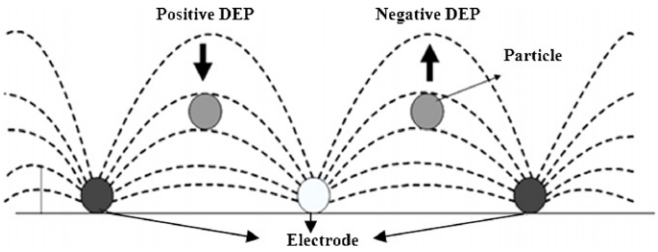

Figure 2. Schematic diagram showing the positive and negative dielectrophoretic forces on particles subjected to non-uniform electric fields.

$$f(\varepsilon_p^*, \varepsilon_m^*) = \frac{\varepsilon_p^* - \varepsilon_m^*}{\varepsilon_p^* + 2\varepsilon_m^*} = \frac{\varepsilon_p - \varepsilon_m - \mathrm{j}\frac{(\sigma_p - \sigma_m)}{\omega}}{\varepsilon_p + 2\varepsilon_m - \mathrm{j}\frac{(\sigma_p + 2\sigma_m)}{\omega}}. \quad (2)$$

For a spherical homogenous particle $f(\varepsilon_p^*, \varepsilon_m^*)$ is referred to as the Clausius–Mossotti factor (C–M factor) [36], where ε_p^* and ε_m^* are the complex permittivities of the particle and medium, respectively, ω is the angular frequency, σ_m and σ_p are the conductivities of the medium and the particle, respectively. It can be seen from the equation that the direction of DEP force is determined by the sign of the real part of the C–M factor which in turn is a function of the frequency of applied field. There is also a cross over frequency setting, $\mathrm{Re}[f(\varepsilon_p^*, \varepsilon_m^*)] = 0$ at which the particle is subjected to zero DEP force. Above the crossover frequency, $\mathrm{Re}[f(\varepsilon_p^*, \varepsilon_m^*)]$ is positive and results in positive DEP, in which force direction is toward higher intensity of electric field, and the particle tends to move toward the region of high field strength. On the other hand, for frequencies below the crossover frequency, $\mathrm{Re}[f(\varepsilon_p^*, \varepsilon_m^*)]$ is negative and leads to negative DEP which applies force toward lower intensity of electric field on the particles and thus they tends to move toward the region of low field strength, as shown in figure 2. Furthermore, in order to generate a non-uniform electric field over the entire height of the channel, electroplated vertical electrodes with a triangular shape embedded in the micro-channel have been designed and fabricated. The frequency of ac E-field is selected such that the particles are subjected to a negative DEP force aligning them into a thin stream at the center.

2.3. Impedance measurements

Traditionally, the MEMS-based Coulter counter employed thin films of electrodes patterned underneath and across the microchannel. This configuration generates non-uniform electric field [13, 37, 38] along the direction of the channel, and most of it is close to its bottom. Thus, those devices measure the impedance along the direction of the channel and generate signal variations if identical particles pass at different heights over the electrodes [13]. In this paper, the Coulter counter is designed with thick electroplated electrodes which will generate a uniform E-field over the entire height of the microchannel along the direction perpendicular to the channel. This will increase the measurement sensitivity. Additionally, multiple pairs of electrodes were spatially distributed throughout the microchannel. Impedance of cells was monitored along the whole channel as cells pass through.

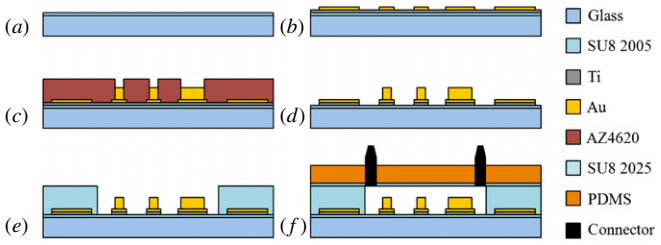

Figure 3. Side view of the Coulter counter fabrication process flow.

3. Design and fabrication

The Coulter counter is designed with three regions, including: (1) multi-fluidic microchannels with passive mixing of the extracellular media, (2) a region for negative dielectrophoretic focusing of the cells and (3) a region containing electrical impedance-based sensing mechanism. The different extracellular media and cells are introduced via two inlets into a Y-shaped channel in the mixing region. This is connected to the focusing region which is connected to the measuring region and on to the outlet. A three-dimensional schematic of the Coulter counter is shown in figure 1. The purpose of this research is to study how cell properties change as a function of time after they are exposed to a certain extracellular media. This is accomplished by placing ten electrode pairs along the Coulter channel such that each electrode pair records the impedance of cell at the time it passes through it. Thus the impedance changes can be tracked as a function of time across the channel. This micro-device is intended to measure the electrical properties of various cell types with diameters ranging from 15 to 20 μm. It consists of a microchannel with a width and depth of 28 μm and 25 μm, respectively. Polydimethylsiloxane (PDMS) is chosen as a cover for the channel, due to its advantages such as flexibility, ease of fabrication and transparency. Since PDMS is a rubber-like material and it highly flexible, it conforms to the curvature of the surface it comes into contact with.

The monolithic fabrication process was used as it lends itself to low-cost manufacturing methods employed in the semiconductor integrated circuit industry. A series of surface micromachining, photolithography, SU-8 photoresist and PDMS processes are employed to fabricate the MEMS Coulter counter (figure 3). The device was fabricated using the following sequence on top of a glass substrate: (1) the glass slides were cleaned in a piranha solution (H_2SO_4: H_2O_2, 3:1) for 3 min and then washed thoroughly with DI water. (2) A thin layer of SU-8 2005 photoresist (MicroChem, Newton, MA) was spin coated onto the glass slides in order to improve the adhesion between the SU-8 channel and glass substrate (figure 3(*a*)). (3) Two layers of titanium (Ti) and gold (Au) were sputter deposited with a thickness of 40 nm and 140 nm, respectively. This layer served as the seed layer for electroplating. A gold layer was patterned and etched using a KI/I_2 solution to create the electrode traces and bonding pads (figure 3(*b*)). (4) A photoresist mold was formed for electroplating the electrodes using an AZ4620

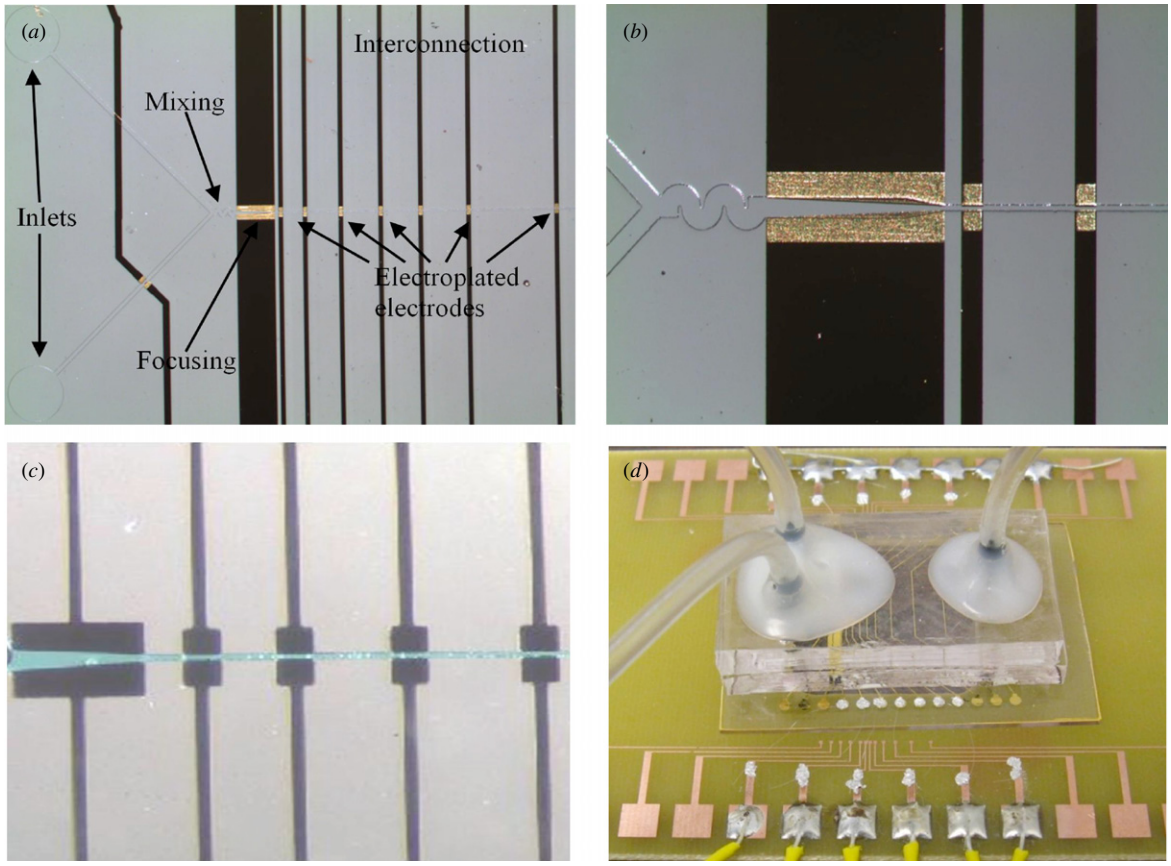

Figure 4. The optical images show: (*a*) the SU-8 channel with the mixing region, focusing electrodes, measuring electrodes, and inlets and outlet (not shown) ports, (*b*) a magnified view of mixing, focusing region and two pairs of electrodes, (*c*) a magnified view of the electrodes and focusing region with a blue dye fluid flowing through the device, (*d*) a complete fabricated and packaged Coulter counter device with PDMS Cover, and fluidic connectors sealed by epoxy glue.

layer with a thickness of 25 μm. The electrodes were formed by electroplating gold (Technic gold 25 ES) inside the mold with a thickness of around 15 μm (figure 3(*c*)). (5) The photoresist was washed away and the Ti layer was wet etched using gold as a mask layer in diluted hydrofluoric acid (figure 3(*d*)). (6) The microchannel was defined using SU-8 2025 with a thickness of 28 μm (figure 3(*e*)). (7) The PDMS slabs (cover) were made and cured to serve as top cover along with fluidic connectors (fluidic inlets and outlets). (8) Oxygen plasma treatment was applied to the PDMS cover in order to change its surface to hydrophilic and then SU-8 2005 was spin coated onto it to serve as glue. The oxygen plasma step was used to improve the adhesion of SU-8 to PDMS. (9) The microchannel was then aligned and bonded to the PDMS cover. The PDMS/SU-8 cover will be cross-linked with the SU-8 microchannel and form a strong bond. (10) The fluidic connectors are further sealed by epoxy glue in order to improve the device reliability. (11) In the last step, the device was fixed and wire bonded to PCB for external electrical connections (figure 3(*f*)). An optical image, magnified view of the fabricated device and a complete device with wire bonding, packaging and soldering for external connections are shown in figure 4.

4. Testing and results

4.1. Mixing of fluids in the channel

Mixing of two reagents in the channel is essential as the experiments are designed to monitor cellular volumetric change after mixing the cell with different extracellular media. Two fluids with different colors are flown from two separate fluid streams using a Y-shape junction and two inlets. One stream contains blue color while the other stream contains only DI water. The volumetric flow rate and pressure in these streams are controlled by a Harvard Apparatus PHD 2000 syringe pump. Once the two color fluids reach the mixing zone, they begin to mix via chaotic and diffusion phenomena. The quality of mixing is evaluated by observing color intensity variation of the two colorful dyes optically as they flow through the mixer and just before they enter into the Coulter channel. It is observed that with a flow rate of 0.4 μl min^{-1}, the two media are mixed sufficiently. As the flow rate increases, the quality of mixing decreases. The mixing of two dyes with different colors in the channel using several flow rates is shown in figure 5. The mixing efficiency was determined by analyzing the captured images, by a CCD camera mounted on an optical microscope and using image processing before and after mixing. The mixing efficiency testing of two media,

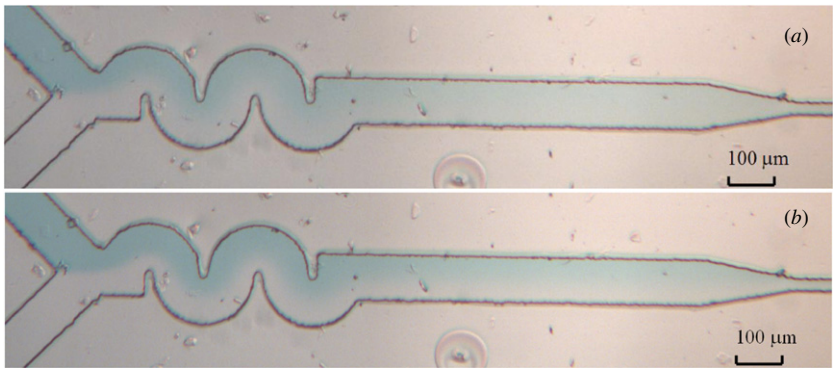

Figure 5. Mixing efficiency testing with different flow rates (*a*) 0.1 μl min^{-1} (*b*) 4 μl min^{-1}.

Table 1. The mixing efficiency was measured as a function of flow rate.

Flow rate (μl min^{-1})	Mixing efficiency (%)
0.1	85
0.4	77
0.8	72
4	50

one with blue color and the other colorless, is shown in figure 4. These images were converted to grayscale images. The intensity of each pixel in the grayscale image represents its level of the blue color. To quantitatively evaluate the mixing efficiency, we will first calculate the standard deviation (σ) at the entrance of the Coulter channel (before the first impedance measurement). Thus, the standard deviation of a narrow strip across the channel at the entrance of the Coulter channel is calculated using Matlab and is given by

$$\sigma = \sqrt{\frac{1}{N}\sum_{i=1}^{N}(I_i - I_{\text{mean}})^2} \tag{3}$$

where I_i and I_{mean} are intensity at the ith pixel and average intensity of the whole narrow strip across the channel, respectively, and N is the total number of pixels within the narrow strip area. The mixing efficiency (C_{mix}) is calculated by normalizing the standard deviation (σ) with respect to the standard deviation at the junction of the two inlets (σ_{inlet}) where no mixing took place [39]:

$$C_{\text{mix}} = \frac{\sigma_{\text{inlet}} - \sigma}{\sigma_{\text{inlet}}} \times 100\%. \tag{4}$$

C_{mix} can be varied from 0% (no mixing) to 100% (complete mixing) and was calculated at the entrance of the Coulter channel for several flow rates as shown in figure 4. The time span between the start of mixing and the first impedance measurement was up to 500 ms. The measured mixing efficiency is shown in table 1. It can be varied from 50 to 85% by varying the fluidic flow rate from 4 to 0.1 μl min^{-1}, respectively. In these experiments, we have used a flow rate of 0.5 μl min^{-1}, which corresponds to a mixing efficiency of 76%. This result shows that there is relatively sufficient amount of mixing by using double serpentine shape passive mixer. The mixing efficiency can be improved by increasing the number of periods or increasing the length of each period of the serpentine shape channel or implementing three-dimensional passive mixing or by using active mixer.

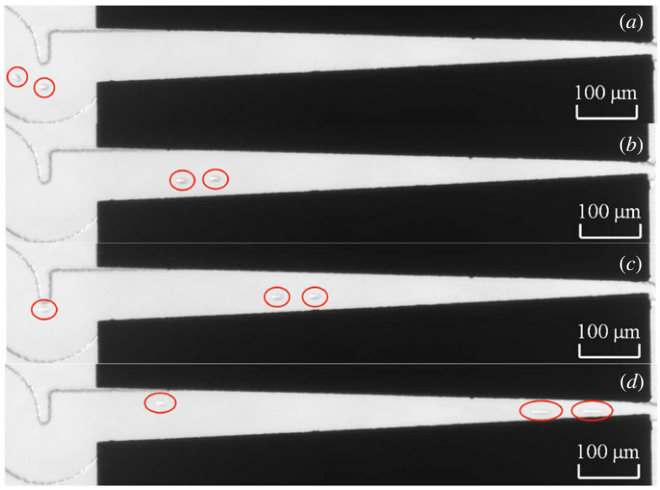

Figure 6. Dielectrophoretic focusing testing (bottom view). Figures are sequential images taken by a CCD camera. There is one moving microbead in each red circle.

4.2. Focusing testing

The focusing region of the device is designed with ramp-up shape electrodes (also called DEP electrodes) in order to focus cells or beads to the center of the microchannel. This is accomplished by applying ac electric field across DEP electrodes. Latex microbeads with a nominal diameter of 10 μm (Beckman Coulter, Miami, FL) in DI water were flown into the microchannel. Figure 6 shows sequential images that demonstrate the movements and focusing of three latex microbeads. The microbeads were focused into the center of the channel when a sinusoid with 6 V peak-to-peak amplitude and 10 MHz frequency was applied to the focusing electrodes. The black areas in the image are bottom views of the DEP electrodes. The microbeads exited the focusing region into the impedance-measuring region on the right-hand side in figure 6(*d*).

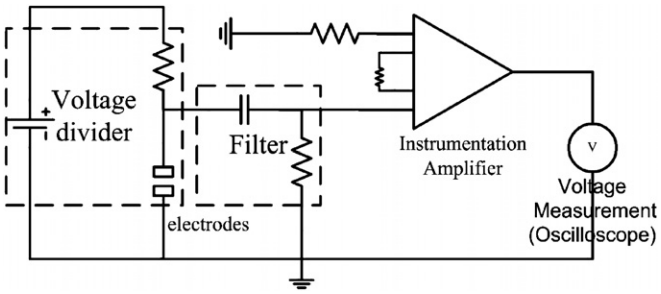

Figure 7. Electrical testing circuit for measuring signal from one channel.

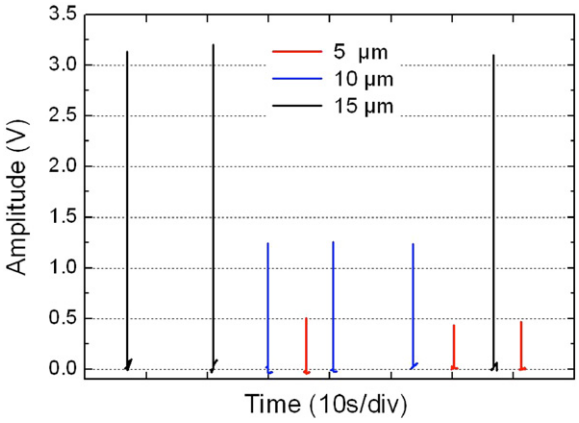

Figure 8. This figure shows voltage pulses with different amplitudes which correspond to microbeads with diameters of 5 μm, 10 μm and 15 μm. The data between pulses were not saved; they were saved only when a pulse is triggered.

4.3. Electrical testing

Prior to assessing the fabricated and packaged Coulter counter devices, an electrical circuit is designed and built in order to measure the resistance changes of microbeads and cells in the measuring region as shown in figure 7. A dc power supply and a resistor with a fixed value are connected to the electrodes to form a voltage divider. The resistance change before and after injecting microbeads in the conductive media, measured by the electrodes can be converted to voltage change. The voltage signal is then passed into a high pass filter in order to block unwanted dc component and then amplified by an instrumentation amplifier and displayed by an oscilloscope. In the case of fibroblast cells, there is no need for signal amplification. We employed Labview system and data acquisition board (DAQ) USB-6216 (National Instrument, Austin, TX) in order to record large volume of data from the multi-channel for analysis and thus enable tracking the impedance of same fibroblast cells by multiple pairs of electrodes as they flow through the microchannel.

The MEMS-based Coulter counter performance was tested by injecting saturated saline water with nominal 5 μm, 10 μm and 15 μm latex microbeads into the microchannel via the two inlets. The measured voltage signals of several microbeads sizes have different amplitudes as show in figure 8. This demonstrates the device ability to differentiate

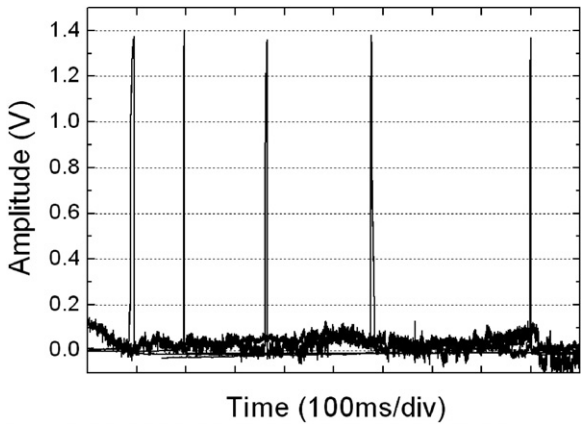

Figure 9. This figure shows voltage pulses of real-time measurement of one fibroblast cell measured by five pairs of electrodes. The five voltage pulses were recorded from five Labview ports and placed together in the same figure for comparison.

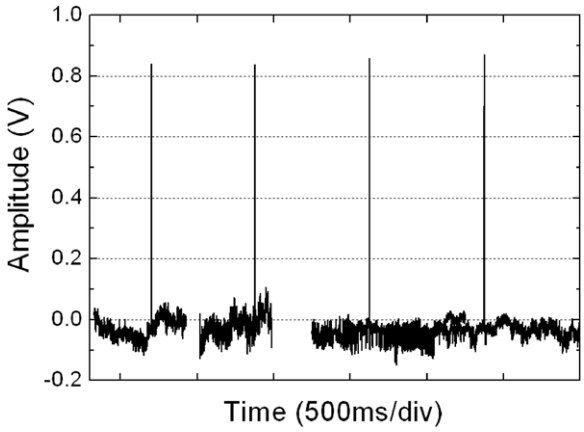

Figure 10. This figure shows voltage pulses of real-time measurement of one fibroblast cell in 0.5× PBS solution measured by four pairs of electrodes. The four voltage pulses were recorded from four Labview ports and placed together in the same figure for comparison. The cells were first in 1× PBS solution and then mixed with DI water in the mixing region to dilute the solution to 0.5× PBS.

between cells and beads based on their size and also count them. The device was also tested using fibroblast cells with a mean diameter of 19 μm and in an isotonic phosphate buffered solution (1× PBS). In the first experiment, fibroblast cells in the 1× PBS solution were injected into the Coulter counter device from both inlets, and the impedance (voltage pulse) of a single cell was recorded in the measuring region using five pairs of electrodes as shown in figure 9. All five pulses have same voltage amplitude as expected since the cell volume would not change. In the second test, the cell changes were recorded as a function of time. In this case, the fibroblast cells in 1× PBS were injected to inlet 1 and deionized water was injected to inlet 2 at the same flow rate. The 1× PBS solution and DI water were mixed in the mixing region and hence the concentration of the solution (mixture) becomes 0.5× PBS in which cells were expected to absorb water and increase their volumes. Figure 10 shows a typical individual cell tracked by four pairs of electrodes. The result showed a slight increase in

amplitude of 0.08 V. In future experiments, the sensitivity of the device will be enhanced by further improving the mixing efficiency.

5. Conclusion

A MEMS Coulter counter device is designed, fabricated and tested. This device uses passive mixing, the phenomenon of negative DEP to focus the cells to the center of the channel and Coulter principle to detect cells based on the change in resistance when they pass through the sensing zone. The fluidic testing, which includes mixing and focusing, demonstrates sufficient mixing and satisfactory focusing. The electrical testing were performed using latex microbeads with diameters of 5 μm, 10 μm and 15 μm, and fibroblast cells (mean diameter 19 μm) with static and dynamic volumes validate the performance of the device.

References

[1] Vellekoop M J and Kostner S 2006 On-chip cell handling and analysis *Proceedings Eurosensors 2006 Keynote Lecture: EUROSENSORS XX, Göteborg, Sweden*

[2] Eastham R D 1963 Rapid whole-blood platelet counting using an electronic particle counter *J. Clin. Pathol.* **16** 168–9

[3] England J M and Down M C 1975 Measurement of the mean cell volume using electronic particle counters *Br. J. Haematol.* **32** 403–10

[4] Levin S W, Levin R L, Solomon A K, Pandiscio A and Kirkwood D H 1980 Improved stop-flow apparatus to measure permeability of human red cells and ghosts *J. Biochem. Biophys. Methods* **3** 255–72

[5] Milgram J H and Solomon A K 1977 Membrane permeability equations and their solutions for red cells *J. Membr. Biol.* **34** 103–44

[6] Larsen D, Blankenstein G and Branebjerg J 1997 Microchip Coulter particle counter *Transducers '97* pp 1319–22

[7] Koch M, Evans A G R and Brunnschweiler A 1999 Design and fabrication of a micromachined Coulter counter *J. Micromech. Microeng.* **9** 159–61

[8] Saleh O and Sohn L 2001 Quantitative sensing of nanoscale colloids using a microchip Coulter counter *Rev. Sci. Instrum.* **72** 4449

[9] Zhe J, Jagtiani A, Dutta P, Jun H and Carletta J 2007 A micromachined high throughput Coulter counter for bioparticle detection and counting *J. Micromech. Microeng.* **17** 304

[10] Ayliffe H E, Frazier A B and Rabbitt R D 1999 Electric impedance spectroscopy using microchannels with integrated metal electrodes *J. Microelectromech. Syst.* **8** 50–7

[11] Rodriguez-Trujillo R, Castillo-Fernandeza O, Garrido M, Arundella M, Valenciac A and Gomilaa G 2008 High-speed particle detection in a micro-Coulter counter with two-dimensional adjustable aperture *Biosens. Bioelectron.* **24** 290–6

[12] Jagtiani A V, Zhe J, Hu J and Carletta J 2006 Detection and counting of micro-scale particles and pollen using a multi-aperture Coulter counter *Meas. Sci. Tech.* **17** 1706–14

[13] Wood D K, Requa M V and Cleland A N 2007 Microfabricated high-throughput electronic particle detector *Rev. Sci. Instrum.* **78** 104301

[14] Morgan H, Sun T, Holmes D, Gawad S and Green N G 2007 Single cell dielectric spectroscopy *J. Phys. D: Appl. Phys.* **40** 61–70

[15] Ateya D A, Erickson J S, Howell P B Jr, Hilliard L R, Golden J P and Ligler F S 2008 The good, the bad, and the tiny: a review of microflow cytometry *Anal. Bioanal. Chem.* **391** 1485–98

[16] Ziaie B, Baldi A, Lei M, Gu Y and Siegel R A 2004 Hard and soft micromachining for BioMEMS: review of techniques and examples of applications in microfluidics and drug delivery *Adv. Drug Deliv. Rev.* **56** 145–72

[17] Tsai C, Hou H and Fu L 2008 An optimal three-dimensional focusing technique for micro-flow cytometers *Microfluid Nanofluid* **5** 827–36

[18] Nieuwenhuis J H, Kohl F, Bastemeijer J, Sarro P M and Vellekoop M J 2004 Integrated Coulter counter based on 2-dimensional liquid aperture control *Sensors Actuators* B **102** 44–50

[19] Lee G, Chang C, Huang S and Yang R 2006 The hydrodynamic focusing effect inside rectangular microchannels *J. Micromech. Microeng.* **16** 1024–32

[20] Gawad S, Schild L and Renaud P 2001 Micromachined impedance spectroscopy flow cytometer for cell analysis and particle sizing *Lab Chip* **1** 76–82

[21] Sundararajan N, Pio M S, Lee L P and Berlin A A 2004 Three-dimensional hydrodynamic focusing in polydimethylsiloxane (PDMS) microchannels *IEEE Trans. J. MEMS* **13** 559–67

[22] Scott R, Sethu P and Harnett C K 2008 Three-dimensional hydrodynamic focusing in a microfluidic Coulter counter *Rev. Sci. Instrum.* **79** 046104

[23] Sun T, Gawad S, Bernabini C, Green N G and Morgan H 2007 Broadband single cell impedance spectroscopy using maximum length sequences: theoretical analysis and practical considerations *Meas. Sci. Technol.* **18** 2859–68

[24] Holmes D, Morgan H and Green N G 2006 High throughput particle analysis: combining dielectrophoretic particle focusing with confocal optical detection *Biosens. Bioelectron.* **21** 1621–30

[25] Chen H T and Wang Y N 2009 Optical microflow cytometer for particle counting, sizing and fluorescence detection *Microfluid Nanofluid* **6** 529–37

[26] Coulter W H 1953 *US Patent* 2656508

[27] Zheng S, Liu M and Tai Y 2008 Micro Coulter counters with platinum black electroplated electrodes for human blood cell sensing *Biomed. Microdevices* **10** 221–31

[28] Coulter W H and Hogo W R 1970 *US Patent* 3502974

[29] Sridhar M, Xu D, Kang Y, Hmelo A B, Feldman L C, Li D and Li D 2008 Experimental characterization of a metal-oxide-semiconductor field-effect transistor-based Coulter counter *J. Appl. Phys.* **103** 104701

[30] Sohn L L, Saleh O A, Facer G R, Beavis A J, Allan R S and Notterman D A 2001 Capacitance cytometry: measuring biological cells one by one *Proc. Natl. Acad. Sci.* **97** 10687–90

[31] Murali S, Xia X, Jagtiani A V, Carletta J and Zhe J 2008 Capacitive Coulter counting: detection of metal wear particles in lubricant using a microfluidic device *Smart Mater. Struct.* **18** 037001

[32] Macknight A D C and Leaf A 1977 Regulation of cellular volume *Physiol. Rev.* **57** 137–54

[33] Yu C, Vykoukal J, Vykoukal D M, Schwartz J A, Shi L and Gascoyne P R C 2005 A three-dimensional dielectrophoretic particle focusing channel for microcytometry applications *IEEE Trans. J. MEMS* **14** 480–7

[34] Zhang C, Khoshmanesh K, Mitchell A and Kalantar-zadeh K 2010 Dielectrophoresis for manipulation of micro/nano

particles in microfluidic systems *Anal. Bioanal. Chem.* **396** 401–20
[35] Çetin B, Kang Y, Wu Z and Li D 2009 Continuous particle separation by size via AC-dielectrophoresis using a lab-on-a-chip device with 3-D electrodes *Electrophoresis* **30** 766–72
[36] Pohl H A 1978 *Dielectrophoresis: The Behavior of Neutral Matter in Non-uniform Electric Fields* (New York: Cambridge University Press)
[37] Wang L, Flanagan L and Lee A P 2007 Side-Wall vertical electrodes for lateral field microfluidic applications *J. Microelectromech. Syst.* **16** 454–61
[38] Gawad S, Schildb L and Renauda P 2001 Micromachined impedance spectroscopy flow cytometer forcell analysis and particle sizing *Lab Chip* **1** 76–82
[39] Nguyen T N T, Kimb M C, Park J S and Lee N E 2008 An effective passive microfluidic mixer utilizing chaotic advection *Sensors Actuators* B **132** 172–81